



Simulation of steel sheet sheathed cold-formed steel framed shear walls

Zhidong Zhang¹, B.W. Schafer²

Abstract

The objective of this paper is to detail the ongoing development and validation of a high fidelity shell finite element model of steel sheet sheathed cold-formed steel (CFS)-framed shear walls. This effort is part of an ongoing research project: CFS-NHERI, which aims to advance the state of the art for seismic performance and design of mid-rise cold-formed steel framed buildings. The strength potential of steel sheet shear walls is large, but the details are critically important. Motivated by the geometry of a tested steel sheet shear wall the ideal capacity of a steel sheet shear wall is simulated and compared against a large variety of available analytical prediction models and testing. The range of potential strength is much greater than in other CFS shear wall systems. Recently, a number of phenomenological performance-based models were developed for CFS-framed shear walls. Although these models are efficient and useful, they typically do not consider buckling of the steel sheet sheathing, nor deformations outside of the localized sheathing-to-chord stud fastener zones, nor cross-section deformations in the cold-formed steel framing, nor stiffness reductions due to local and/or distortional buckling of the stud or track. All of these aspects can be incorporated in a more general modeling framework as implemented in a predominately shell finite element-based model. Both single steel sheet sheathed and double steel sheet sheathed shear wall models are examined herein. CFS members and the steel sheet sheathing are modeled with shell elements while sheathing-to-frame fasteners are modeled with springs. The developed models are being validated against available test data and show promise, but more work is required before the models can be considered complete. The models will be used to predict and augment ongoing and future testing in the CFS-NHERI project and to conduct parametric studies to determine improved details and performance.

1. Introduction

Cold-formed steel (CFS)-framed structures have potential for low installation and maintenance costs, are lightweight and recyclable, and properly designed are durable, and ductile. Moreover, the high strength-to-weight ratio, stiffness, dimensional consistency, and non-combustibility of CFS affords the system potential benefits over certain aspects of competing solutions. CFS-framed mid-rise structures have the potential to fulfill the need for low cost, multi-hazard resilient, sustainable building structures.

¹ Graduate Research Assistant, Dept. of Civil Engineering, Johns Hopkins University, <zhidongzhang@jhu.edu >

² Professor, Dept. of Civil Engineering, Johns Hopkins University, <schafer@jhu.edu>

However, limitations in the available research and in design guidance for the seismic response of mid-rise CFS-buildings at component, subsystem, and full-scale building levels are a barrier to substantiating performance and bringing the potential benefits to the built infrastructure. The efforts reported here are part of an ongoing research project: CFS-NHERI. This project aims to advance the state of the art for seismic performance and design of mid-rise CFS-framed buildings. Strap braced shear walls, wood sheathed shear walls, and steel sheet sheathed shear walls are typical lateral force resisting systems in CFS-framed structures. Steel sheet sheathed shear walls have demonstrated strong potential for higher capacities necessary in mid-rise construction. CFS-framed steel sheet shear walls consist of studs, tracks, and bridging members fastened together along with steel sheet sheathing on one or both sides of the framing. This paper summarizes current experimental and simulation work related to CFS-framed shear walls, specifically explores the bounds on steel sheet shear walls, and provides the initial development of a high fidelity shell finite element model for CFS-framed steel sheet sheathed shear walls.

2. Available Experiments

A significant number of single story monotonic and reversed cyclic tests have been conducted on CFS-framed shear walls. Recently a database of available tests was compiled and now includes 700 CFS-framed shear wall tests assembled from 29 primary references (Ayhan et al. 2018). This database details major features of the tested specimens and also provides the complete load-displacement response of both monotonic and reversed cyclic (static) tests conducted over approximately the last 20 years. To date the database has been used to develop ASCE 41 modeling protocols, and to better understand the expected strength and reliability and resistance (safety) factors appropriate for CFS-framed shear walls.

CFS-framed shear wall experimental work initiated with Serrette et al. (1997) and resulted in the first design standards for CFS-framed wood-sheathed shear walls. Rogers and his research team extended these shear wall tests to incorporate various sheathing and framing details (Branston et al. 2006), CFS-framed steel strap shear walls (Al-Kharat et al. 2007), steel sheet sheathed shear walls (Ong-Tone et al. 2009, Balh et al. 2010 & 2014, DaBreo et al. 2012), and pseudo-dynamic tests on two-story steel sheet sheathed shear walls (Shamim et al. 2013). Yu and his team also expanded the research work on steel sheet sheathed shear walls (Yu et al. 2007 & 2010).

Recently Rogers and his students have developed new steel sheet sheathed shear wall configurations to achieve higher strength (than currently available in AISI S400-16) and ductility to resist the larger demands expected in mid-rise construction. Rizk & Rogers (2017) adopted thicker framing components and also used full blocking reinforcement (quarter point blocking) while Santos & Rogers (2017) and Briere & Rogers (2017) developed double sheathed and mid-ply sheathed steel sheet sheathed shear wall configurations. To understand the effects of architectural finishes and different framing systems along the same lateral force resisting wall line, the ongoing CFS-NHERI project recently conducted a series of dynamic test on 7.6m (16 ft) long portions of CFS-framed walls with 1.9 m (4 ft) segments of steel sheet sheathed shear walls. At the same time, there is a high demand for simulation work to explore new designs and help to determine improved details and performance.

3. Modeling Approaches

Significant modeling work has been completed to investigate CFS-framed shear wall behavior. The most common strategy for shear wall modeling is phenomenological and seeks to reproduce the fundamental shear force-displacement response of the walls including strength degradation and pinching under hysteretic demands. Two common phenomenological modeling strategies are presented in Fig. 1. Examples of this approach include Blais (2006) models of CFS-framed OSB sheathed shear walls using nonlinear diagonal trusses implemented in Ruaumoko. Similarly, Kechidi & Bourahla (2016) adopted nonlinear zero length elements connected to rigid truss elements to replicate the hysteretic behavior of CFS-framed wood and steel sheet sheathed shear walls. Leng (2017) also implemented a similar model with nonlinear diagonal truss elements in his “state-of-the-practice” CFS-framed wood-sheathed shear wall model in OpenSees. Yu (2015) also put forward a similar model for CFS-framed corrugated steel sheet sheathed shear walls simulated in OpenSees. Comeau (2008) modeled CFS-framed weld-connected strap-braced shear walls in Ruaumoko featuring bi-linear spring elements along the two strap directions.

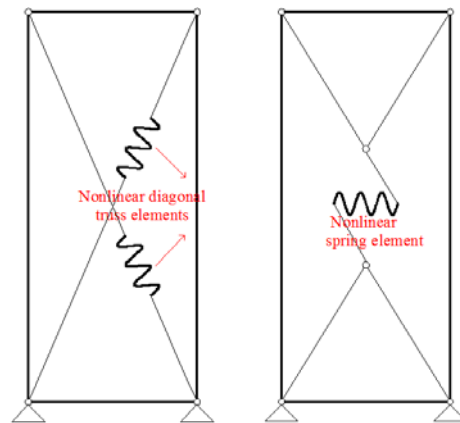


Figure 1: Two common phenomenological modeling strategies

Although a phenomenological, or behavior-based, modeling strategy is efficient the approach is limited to the behavior captured in the underlying testing. If an actual wall in a building experiences different levels of gravity load, interacts with attached framing at any level other than the floor, or engages limit states not observed in the testing these contributions will be excluded in the phenomenological model. In many cases critical aspects of the mechanical performance of the wall can be explicitly simulated. Such an explicit, or mechanics-based, modeling strategy may be implemented in more robust finite element platforms using shell elements and material and geometric nonlinearity, as implemented in ABAQUS or ANSYS and depicted in Fig. 2. This modeling framework simulates explicitly the CFS members, strap braces, sheathing components, etc. For example, Hung (2014) modeled CFS-framed wood sheathed shear walls in ABAQUS using S4R shell elements and nonlinear springs for fasteners. Zeynalian (2012 & 2015) modeled CFS-framed steel strap-braced and steel sheet sheathed shear walls using SHELL181 (shell) elements and COMBIN39 (spring) elements in ANSYS.



Figure 2: Explicit (detailed) modeling strategy

Modeling strategies also may be mixed including both phenomenological and explicit mechanics-based approaches. For example, Buonopane et al. (2015) proposed a fastener-based model in OpenSees to simulate CFS-framed wood sheathed shear walls. In this model, the hysteretic response of individual fasteners in shear are implemented directly at the actual fastener locations, but other elements in the wall remain elastic or rigid, see Fig. 3. This approach allows for fastener spacing and response to be varied and for more complex load distributions on the perimeter of the wall – but does not include all possible limit states for the wall. There are also some other mixed modeling strategies, e.g. considering the subdivision of the sheathing board as subpanels or simulating the steel sheet as truss brace net, as presented in Fig. 4. Leng (2017) proposes a state-of-the-art CFS-framed wood sheathed shear wall model in OpenSees for the CFS-NEES project which subdivided the sheathing board into subpanels thus explicitly considering ledger, window or door headers’ in generating secondary shear load paths. The model used diagonal trusses with Pinching4 uniaxial material to simulate the hysteretic behaviors. Shamin & Rogers (2013) modeled steel sheet sheathed CFS-framed shear walls in OpenSees. In their model, the sheathing board panel is modeled as a net of truss braces with the Pinching4 material replicating the shear wall inelastic behaviors and the chord studs or tracks are simulated as elastic beam-column elements.

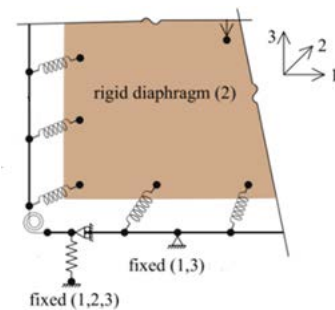


Figure 3: Mixed modeling strategy (more explicit)

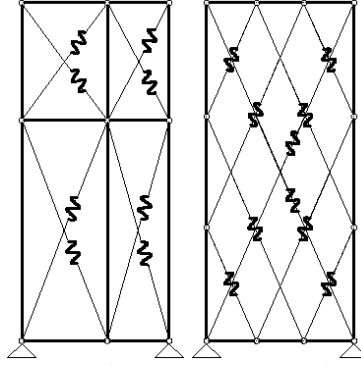


Figure 4: Mixed modeling strategy (more phenomenological)

Application of explicit modeling strategies have seen relatively limited use. Given the potential strength benefits of higher capacity, more ductile, steel sheet sheathed shear walls further development of this approach is needed. High fidelity finite element simulations are needed to explore and improve new steel sheet shear wall designs and better understand their performance and interaction with the surrounding framing. To consider deformation and buckling of the steel sheet sheathing and nonlinear deformation in the framing components, this paper will put forward developments towards an explicit (high fidelity) shell finite element model in ABAQUS appropriate for steel sheet sheathed CFS-framed shear walls. It is worth noting that recently Mojtabaei (2018) provided a similar summary of CFS shear wall modeling.

4. Bounds and Strength Models for Steel Sheet Sheathed Shear Walls

Steel sheet shear walls are unusual in that the range of potential strength between elastic buckling of the thin steel sheet and gross yielding of the sheet is large. Consider a typical $a = 1.22 \text{ m} \times h = 2.44 \text{ m}$ (4 ft x 8 ft) $t = 0.76 \text{ mm}$ (0.03 in.) steel sheet with $F_y = 333 \text{ MPa}$ (48.30 ksi), $E = 2.03 \times 10^5 \text{ MPa}$ (29500 ksi), $\nu = 0.3$, as employed in test W2 of Rizk and Rogers (2017). For the W2 test the peak shear strength $V_{test} = 48 \text{ kN}$ (11 kips). For an estimate of the upperbound gross yield strength we may treat the sheet the same as a web in a conventional member, thus per AISI S100-16 (2016) the sheet yield strength V_y :

$$V_y = A_w \tau_y \quad (1)$$

where A_w is the cross-section of the sheet (ht) and τ_y is the yield stress in shear:

$$\tau_y = 0.6F_y \quad (2)$$

where F_y is the yield stress in tension and h is the height of the steel sheet and t is the thickness. For the W2 specimen $V_y = 200 \text{ kN}$ (45 kips).

For an estimate of the critical elastic buckling strength, V_{cr} , we again treat the sheet as a deep web and employ AISI S100-16 (2016):

$$V_{cr} = A_w \tau_{cr} \quad (3)$$

Where A_w is the area of cross-section of the sheet (ht) and the shear buckling stress is defined as:

$$\tau_{cr} = k_v \frac{\pi^2 E}{12(1-\nu^2)} \left(\frac{t}{h}\right)^2 \quad (4)$$

$$k_v = 4.00 + \frac{5.34}{(a/h)^2} \quad \text{when } a/h \leq 1.0$$

$$k_v = 5.34 + \frac{4.00}{(a/h)^2} \quad \text{when } a/h > 1.0 \quad (5)$$

Where E is the elastic modulus of the steel sheet, ν is the Poisson's ratio of the steel sheet, and a is the sheet width. For the W2 specimen $V_{cr} = 2.33$ kN (0.52 kips) if we take h as half of the sheet height considering the field stud as a transverse stiffener. It is possible to consider using blocking or other detailing to further break up the shear buckling (and change the a/h ratio); however, even with these changes V_{cr} is remarkably low for such a thin steel sheet. With such large bounds in potential response a large variety of methods have been developed to provide estimates of the strength capacity of steel sheet. Several of these methods are detailed in the following to provide an appreciation for the wide range of potential strength predictions.

For example the SSRC Design Guide (Ziemian 2010) provides an upperbound estimate for sheet with rigid edge boundaries that relies on tension field action, in this approach:

$$V_{nSSRC} = \tau_{cr} ht + \frac{1}{2} \sigma_{ty} ht \quad (6)$$

$$\sigma_{ty} = \sqrt{F_y^2 - 0.75\tau_{cr}^2} - 1.5\tau_{cr} \quad \text{provided that } \tau_{cr} \ll F_y \quad (7)$$

For the W2 specimen $V_{nSSRC} = 174$ kN (39 kips), which is relatively close to the upperbound yield capacity and greatly in excess of the tested capacity.

Alternatively we may adapt AISC 341-10 (2010) which provides a nominal strength prediction for steel plate shear walls, $V_{nAISC341}$ in accordance with the limit state of shear yielding:

$$V_{nAISC341} = 0.42F_y ht \sin 2\alpha \quad (8)$$

where α is the angle of web yielding in degrees as measured relative to the vertical, which is permitted to be taken as 40 degrees or calculated using the formula listed in F5.5b in AISC 341-10 (2010). For the W2 specimen $V_{nAISC341} = 143$ kN (32 kips), which is relatively close to the SSRC infinite boundary condition capacity.

AISC 360-10 (2010) provides the nominal shear strength $V_{nAISC360}$ of a steel plate girder with tension field action, this can provide an additional estimate of the strength:

$$\begin{aligned}
(a) \quad V_{nAISC360} &= 0.6F_y A_w && \text{when } h/t \leq 1.10\sqrt{k_v E / F_y} \\
(b) \quad V_{nAISC360} &= 0.6F_y A_w \left(C_v + \frac{1 - C_v}{1.15\sqrt{1 + (a/h)^2}} \right) && \text{when } h/t > 1.10\sqrt{k_v E / F_y}
\end{aligned} \tag{9}$$

k_v determined as below:

(i) For webs without transverse stiffeners and with $h/t < 260$:

$$k_v = 5.00$$

except for the stem of tee shapes where $k_v = 1.2$

(ii) For webs with transverse stiffeners:

$$\begin{aligned}
k_v &= 5.00 + \frac{5.00}{(a/h)^2} \\
&= 5.00 \quad \text{when } a/h > 3.0 \text{ or } a/h > \left[\frac{260}{(h/t)} \right]^2
\end{aligned}$$

C_v determined as below:

(i) When $h/t \leq 1.10\sqrt{k_v E / F_y}$:

$$C_v = 1.00$$

(ii) When $1.10\sqrt{k_v E / F_y} < h/t \leq 1.37\sqrt{k_v E / F_y}$:

$$C_v = \frac{1.10\sqrt{k_v E / F_y}}{h/t}$$

(iii) When $h/t > 1.37\sqrt{k_v E / F_y}$:

$$C_v = \frac{1.51k_v E}{(h/t)^2 F_y} \tag{10}$$

k_v is the AISC specific web plate shear buckling coefficient and C_v is the web shear coefficient. For the W2 specimen $V_{nAISC360} = 81$ kN (18 kips), which is significantly below the pure tension field action cases, but still well above the tested capacity.

AISI S400-15 (2015) provides an empirically calibrated effective strip (“tension field”) method, which could predict the nominal shear strength limited by sheathing yield capacity, $V_{nAISIS400}$.

$$V_{nAISIS400} = 1.33w_e t F_y \cos \alpha \tag{11}$$

$$\begin{aligned}
\alpha &= \text{Arctan}(a/h) \\
w_e &= w_{\max}, \text{ when } \lambda \leq 0.0819 \\
&= \rho w_{\max}, \text{ when } \lambda > 0.0819 \\
&\text{where } w_{\max} = h / \sin \alpha \\
\rho &= \frac{1 - 0.55(\lambda - 0.08)^{0.12}}{\lambda^{0.12}} \\
\lambda &= 1.736 \frac{\alpha_1 \alpha_2}{\beta_1 \beta_2 \beta_3^2 (a/h)} \tag{12} \\
&\text{where} \\
\alpha_1 &= F_{ush} / 310.3(\text{MPa}) \text{ or } F_{ush} / 45(\text{ksi}) \\
\alpha_2 &= F_{uf} / 310.3(\text{MPa}) \text{ or } F_{uf} / 45(\text{ksi}) \\
\beta_1 &= t / 0.457(\text{mm}) \text{ or } t / 0.018(\text{inch}) \\
\beta_2 &= t_f / 0.457(\text{mm}) \text{ or } t_f / 0.018(\text{inch}) \\
\beta_3 &= s / 152.4(\text{mm}) \text{ or } s / 6(\text{inch})
\end{aligned}$$

where F_{ush} , F_{uf} , t_f , and s are the tensile strength of steel sheet sheathing, minimum tensile strength of framing materials, minimum design thickness of framing members, and screw spacing on the panel edges, respectively. For the W2 specimen $V_{nAISIS400} = 82.50$ kN (18.54 kips).

In addition to the analytical methods a simplified FE model was developed to investigate the behavior of the steel sheet. The model uses shell finite elements for the sheet, but pin-connected rigid beam elements for the framing. Elastic buckling of the model is explored, and the first mode is shown in Fig. 5, and found to be numerically the same as the analytical V_{cr} . (Eq. 3 = 2.33 kN, simulation = 2.34 kN). The sheet is also modeled as elastic-perfectly plastic to explore its upperbound strength. Although the boundary is rigid, the attachment pattern on the perimeter is the same as the W2 test (i.e. attached every 50.8 mm). In this case the attachments are idealized as perfect pins using MPC constraints in ABAQUS. The response of the model is provided in Fig.6. The response of the simulation, the selected test, and all of the predictions for test W2 are provided in Fig. 7. The difference between the idealized ‘‘ABAQUS Nonlinear Analysis’’ is due to (a) additional deformation at the fastener locations, and (b) the effect of non-rigid boundary members.

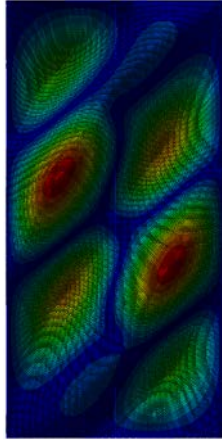


Figure 5: First order buckling mode of the ideal FE ABAQUS model of W2 shear wall

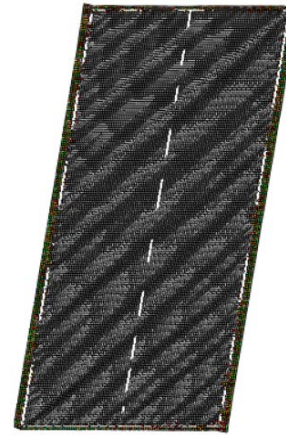


Figure 6: Deformation pattern of the nonlinear analysis of the ideal FE ABAQUS model of W2 shear wall

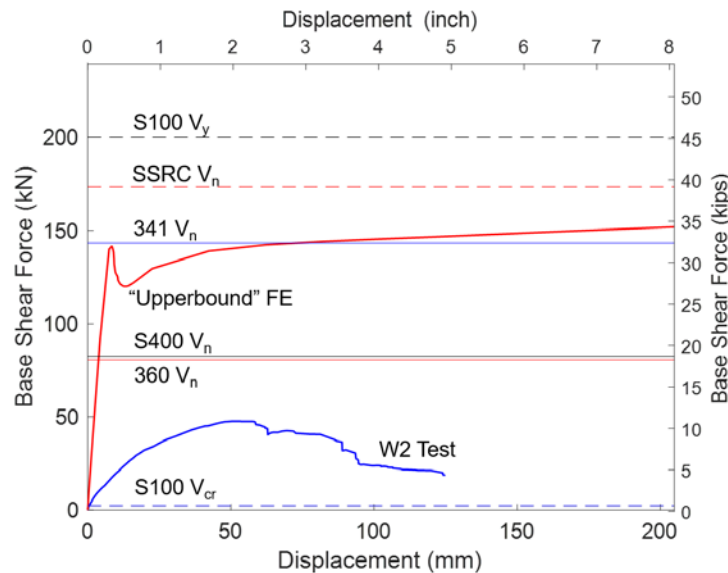


Figure 7: Shear strength comparison between test result and ideal strength model simulation result and code predictions for W2 shear wall

In comparing the solutions of Fig. 7 one can gain an understanding of the sensitivity and complication of CFS-framed steel sheet shear walls. Sheet post-buckling is so extensive that elastic critical buckling is almost irrelevant to understanding the response. Gross sheet yielding is equally limited in its applicability since yielding only occurs in regions of the shear buckled sheet. Ideal capacities (such as the ABAQUS model or the AISC 341 steel plate shear wall) may be up to 3 times greater than tested capacity. Ideal capacities may only be developed with rigid boundary members. So CFS framing (flexibility) plays a prominent role in the strength of CFS-framed steel sheet shear walls – and this negates some of the potential benefits of the system at this time.

The sensitivity of steel sheet shear walls is an indication that the modeling task will not be simple if all of the mechanics is to be captured. At the same time, the potential benefits are great since currently only testing is capable of predicting steel sheet shear walls that attempt to more completely utilize the potential capacity of the system.

5. High Fidelity Shell Finite Element Model of Single Steel Sheet Shear Wall

The aim of current efforts is to develop an accurate and robust set of modeling protocols for explicit/mechanics-based modeling of CFS-framed steel sheet shear walls. A high fidelity shell finite element model is being developed in ABAQUS for this purpose. The work is underway, and current progress is reported herein.

5.1 Specimen Details

The initial target experiment is the 1.22 m x 2.44 m (4 ft x 8 ft.) steel sheet shear wall designated as W2 and tested and reported in Rizk and Rogers (2017). This wall was also utilized to motivate details in recent dynamic wall-line tests conducted as part of the CFS-NHERI effort. As summarized in Fig. 8, the W2 test specimen is a CFS-framed shear wall composed of back-to-back chord studs, top and bottom tracks, quarter point channel blocking tracks, steel sheet sheathing on one side and four Simpson Strong-Tie S/HD 10S hold downs, per Rizk and Rogers (2017). Material properties for each member are provided in Table 1.

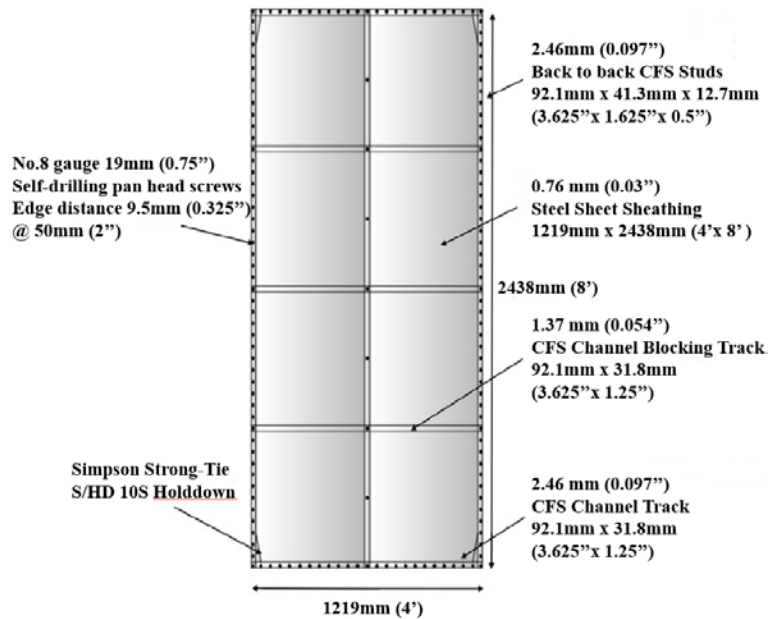


Figure 8: W2 (single sheathed) shear wall member information

Table 1: W2 shear wall material properties

Member	Yield Stress F_y (MPa)	Tensile Stress F_u (MPa)	F_u/F_y
Stud	370 (53.7 ksi)	450 (65.3 ksi)	1.22
Track	341 (49.5 ksi)	427 (61.9 ksi)	1.25
Sheathing	333 (48.3 ksi)	406 (58.9 ksi)	1.21

5.2 Model Details

The stud, track and sheet are modeled with the 8-node doubly curved reduced integration shell element (S8R) in ABAQUS. For developing the structured mesh for each part, as shown in Fig. 9, a global seed size of 12.7 mm (0.5 inch) is employed. For the rounded corner areas in the studs and track, 4 elements are meshed in the curvature direction.

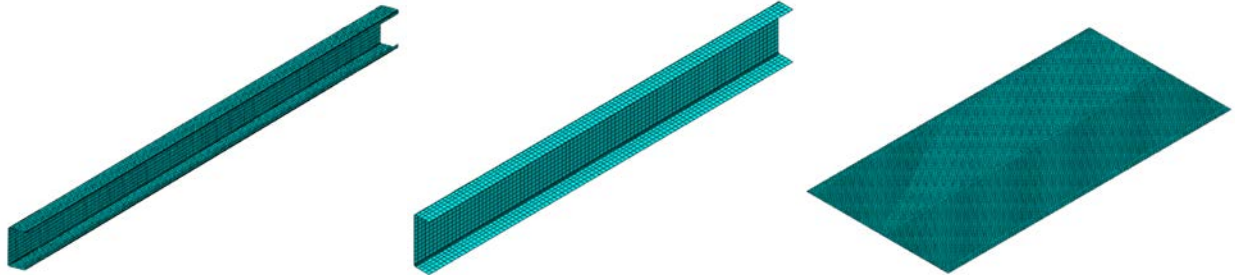


Figure 9: Mesh arrangements of studs, tracks and sheet in the ABAQUS model

The stud-to-track connections, blocking track-to-stud connections, and connections between the back-to-back chord studs are modeled as pin connections using multi-point constraints (PIN_MPC), indicated as green characters ‘MPC PIN’ in Fig. 10. In addition, a key challenge in this high fidelity ABAQUS modeling strategy is the modeling of the fastener connecting the sheathing to the framing components. Different from the idealized connections used elsewhere, horizontal and vertical linear elastic springs together with fixed coupling in the out-of-plane direction are combined to simulate the fastener behavior, as indicated by the pink points in Fig. 10 and presented in detail in Fig. 11. The fastener stiffness is established from the fastener backbone strength and stiffness equations regressed based on test data in Tao and Moen (2016). The hold downs are simulated as nonlinear elastic connector elements whose negative (bearing) stiffness is 1000 times larger than the positive (tension) stiffness (which is based on available tests). Further, the face along the chord stud web in contact with the hold down is assumed to be connected.

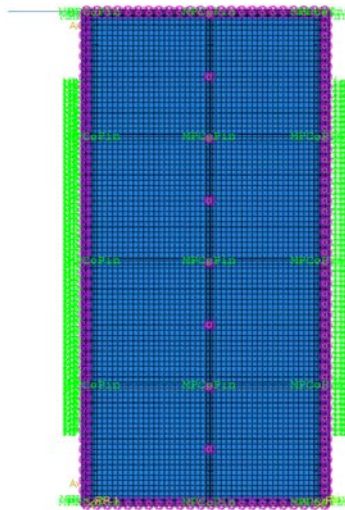


Figure 10: Interaction settings in the W2 shear wall ABAQUS model

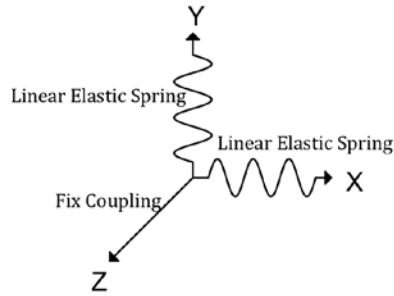


Figure 11: X & Y direction linear elastic springs and Z direction fix coupling for fastener modeling

To simulate the actual test configuration, a rigid beam element simulating the load beam is incorporated into the model, which is presented as a blue line extending from the left at the top of the shear wall in Fig. 10. The load is applied to the left end of the rigid beam and the rotation degree of freedom of the load beam is constrained at its middle point.

Eigenvalue buckling analysis of the model is conducted to introduce imperfections of a magnitude of $1.0t$ in the steel sheet. The dynamic implicit solver is employed in ABAQUS together with the application of a monotonic constant slow velocity lateral movement. This has been found to generate better convergence performance than the static general solver for this model. Additionally, the anchors connecting the bottom track to the ground are simulated as translational boundary conditions (fixed in all three translational degree of freedoms) and the anchors connecting the top track to the load beam are modeled with multi-point constraints (PIN_MPC). Out-of-plane support of the test frame is treated as a boundary condition – as the out-of-plane degree of freedom along the load beam is fixed.

5.3 Preliminary Results

According to Rizk and Rogers (2017), the W2 shear wall test specimen's failure behavior and deformation pattern features flange and lip distortion of the chord studs, uplift of the bottom track, and pull through of the fasteners in the steel sheet sheathing. In assessing the performance of the model we must first note that pull through is not captured in the model created to date. The chord studs in the model do exhibit similar distortions as reported in the testing and shown in Fig. 12. The model also predicts significant uplift of the bottom track as shown in Fig. 13. However, large difference exists between the test and simulation shear-deformation response as provided in Fig. 14.

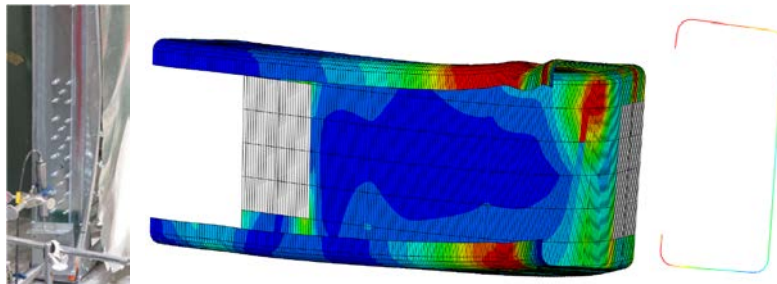


Figure 12: Comparison of left chord stud deformation between test and simulation for W2 shear wall

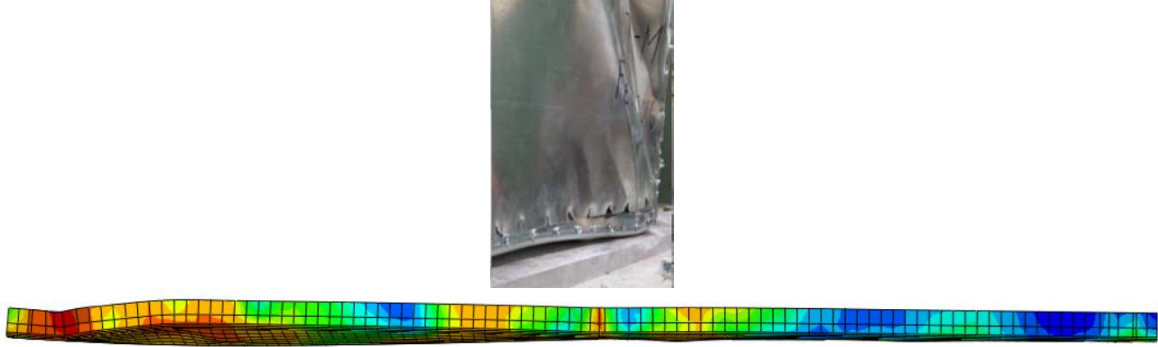


Figure 13: Comparison of track deformation between test and simulation for W2 shear wall

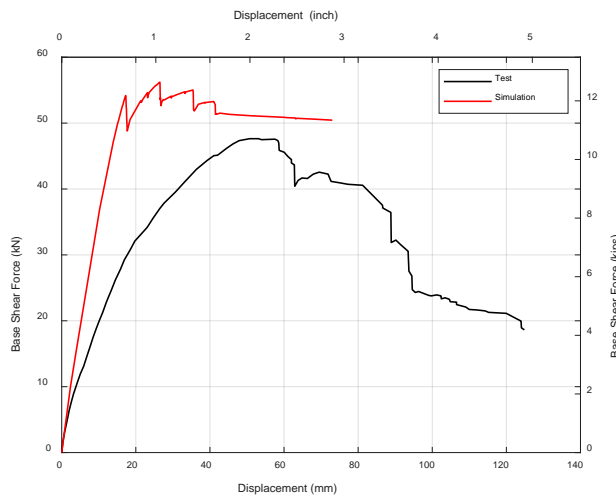


Figure 14: Comparison of lateral load-displacement curves between test and simulation for W2 shear wall

Overall the model is too stiff, too strong, and too slow to demonstrate degrading stiffness. In the context of Fig. 7 the predicted performance has some merit – clearly the impact of the framing is being included at some level. The working hypothesis is that the sheet-to-framing fasteners must use a more sophisticated model and the other steel-to-steel connectors may also need to have flexibility introduced into the model. We are investigating a variety of methods to incorporate more sophisticated fastener modeling at this time.

6. High Fidelity Shell Finite Element Model of Double Steel Sheet Shear Wall

6.1 Specimen Details

Specimen W21 from Santos and Rogers (2017) as depicted in Fig. 15 is selected for additional study. This 1.22 m x 2.44 m (4 ft x 8 ft) double-sided steel sheet shear wall exhibited significant capacity, but still generally follows conventional CFS-framed detailing.

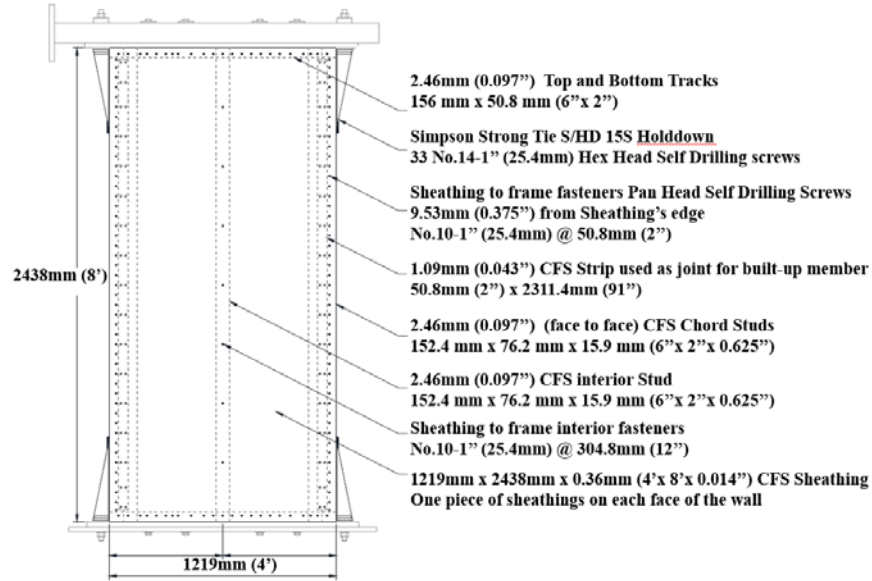


Figure 15: W21 (double sheathed) shear wall member information

The chord studs are boxed (toe-to-toe) to provide increased torsional resistance against the large forces developed at the steel sheet-to-chord stud fastener locations. The specimen uses conventional top and bottom track and hold downs. Material properties are provided in Table 2.

Table 2: W21 shear wall material properties

Member	Yield Stress Fy (MPa)	Tensile Stress Fu (MPa)	Fu/Fy
Stud	389 (56.4 ksi)	461 (66.9 ksi)	1.19
Track	380 (55.1 ksi)	451 (65.4 ksi)	1.19
Sheathing	324.5 (47.1 ksi)	364 (52.9ksi)	1.12

6.2 Model Details

Similar to the single steel sheet shear wall model, the SR8 shell element is adopted and a global mesh seed size is chosen as 12.7 mm (0.5 inch) for the studs, tracks, and steel sheet. At least four elements are used in corner regions of the stud and track. Stud-to-track connections and the connection locations for the face-to-face chord studs are modeled as pin connections using multi-point constraints, as indicated by the green 'MPC PIN' designation in Fig. 16. The horizontal and vertical linear elastic springs together with fixed out-of-plane coupling is employed to simulate the fasteners connecting the sheathing to the framing components, as indicated by the pink points in Fig. 16. Again the fastener stiffness is determined based on Tao and Moen (2016). The hold downs are simulated with tested stiffness in tension and rigid (1000X) stiffness in bearing. All faces along the stud web in contact with the hold downs are modeled as rigid bodies, see the yellow areas in Fig. 16. The loading beam is modeled the same as in the previous model.

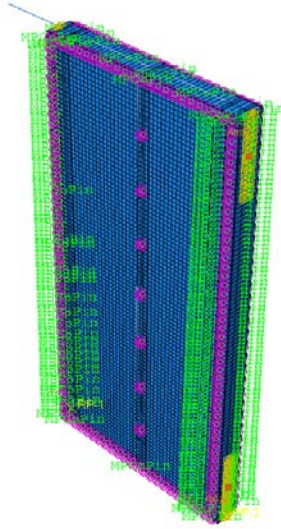


Figure 16: Interaction settings in the W21 shear wall ABAQUS model

The anchors connecting the bottom track to the ground are simulated as fixed in translation and the anchors connecting the top track to the load beam are modeled with multi-point constraints. The load beam is supported out-of-plane. Eigenvalue buckling analysis is used to generate an imperfection pattern in the steel sheet and scaled to 1.0t. The dynamic implicit solver is employed as a small velocity is imparted in the model.

6.3 Preliminary Results

The W21 shear wall test specimen's primary behavior features sheet buckling and bearing and pull through of the connectors for the steel sheet sheathing (Santos and Rogers 2017). The response of the ABAQUS simulation is shown in Fig. 17 and plotted against the test load-deformation response in Fig. 18. The overall behavior of the model is promising, initial stiffness is reasonable and the response of the steel sheet (Fig. 17) is qualitatively similar to that observed in the testing. It appears that the more robust chord stud detail is at least partially successful as the stiffness of the tested wall does not degrade at relatively low load levels. Inability to accurately capture the fastener-based pull through limit state again leads to inadequacy in the model. As reported in Fig. 18 the convergence criteria were relaxed to establish a peak capacity from the available model. Without the fastener failure mode the strength is over-predicted by 27% in the current model. More accurate simulation of the fastener response is needed.

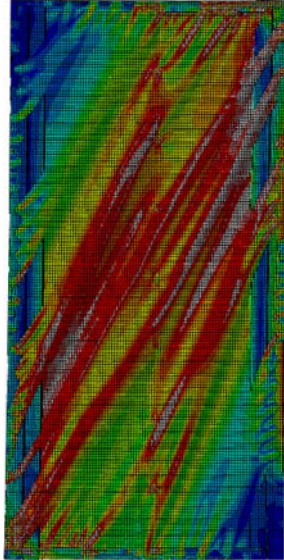


Figure 17: Deformation pattern of W21 shear wall in ABAQUS nonlinear analysis

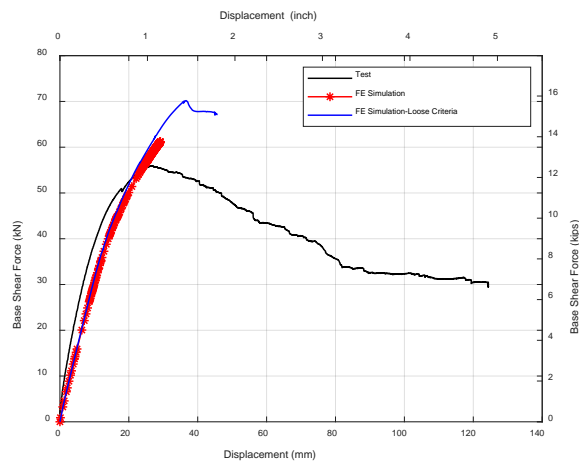


Figure 18: Comparison of the lateral load-displacement curves between test and simulations for W21 shear wall

7. Future Work

The aforementioned simulation work is challenging and not yet fully successful in capturing the main specimen characteristics for higher capacity steel sheet shear walls. We are working on adopting suitable nonlinear connector elements for the fastener behavior modeling to continue the development, validation, and application of this high fidelity shell finite element model. Additionally, a center-sheathed shear wall model will also be developed. Moreover, both displacement-based monotonic and cyclic lateral load will be applied to these models so that they can be used for the prediction of lateral response of steel sheet sheathed CFS-framed shear walls and wall lines including the ongoing and future testing in the CFS-NHERI project. Finally, the models are intended for parametric studies to determine improved details and performance of steel sheet sheathed CFS-framed shear walls.

8. Conclusions

Cold-formed steel (CFS)-framed steel sheet shear walls have significant potential to provide increased strength and ductility necessary for mid-rise CFS construction. However, the response of these systems is sensitive to the boundary conditions of the wall and current detailing provides sub-optimal strength and ductility. Analytical and finite element models indicate that capacities for steel sheet sheathed shear walls could readily be tripled if the boundary behavior is improved and fastener limit states avoided. To further explore this behavior and potential gains in strength and ductility a high fidelity nonlinear shell finite element model of CFS-framed steel sheet shear walls is developed. The model captures the flexibility of the boundary members, even under relatively complex loading, but due to simplified models currently used for the sheet-to-stud connection is unable to accurately predict peak strength and post-peak response. At this time the model still requires further development, and options for integrating the nonlinear fastener response are currently being explored. The intent of the developed models is to explore and optimize the potential for CFS-framed wall lines that employ steel sheet for lateral resistance.

Acknowledgments

This work was supported in part by the National Science Foundation under Grant No. 1663348. Any opinions expressed in this paper are those of the authors alone, and do not necessarily reflect the views of the National Science Foundation.

References

- Ayhan, D., Baer, S., Zhang, Z., Rogers, C. A., Schafer, B.W. (2018). "Cold-Formed Steel Framed Shear Wall Database." *Proceedings of Wei-Wen Yu International Specialty Conference on Cold-Formed Steel Structures 2018*, St. Louis MO. 599-613.
- Serrette, R., Encalada, J., Hall, G., Matchen, B., Nguyen, H., Williams, A. (1997). "Additional Shear Wall Values for Light Weight Steel Framing." Light Gauge Steel Research Group, Report No. LGSRG-1-97, Santa Clara University. Santa Clara, CA, USA.
- Serrette, R.L., Morgan, K.A., Sorhouet, M.A. (2002). "Performance of Cold-Formed Steel-Framed Shear Walls: Alternative Configurations." Light Gauge Steel Research Group, Report No. LGSRG-06-02, Santa Clara University. Santa Clara, CA, USA.
- Serrette, R., Nguyen, H., Hall, G. (1996). "Shear Wall Values for Light Weight Steel Framing." Light Gauge Steel Research Group, Report No. LGSRG-3-96, Light Gauge Steel Research Group, Department of Civil Engineering, Santa Clara University. Santa Clara, CA, USA.
- American Iron and Steel Institute (AISI) (2007). "AISI S213-07, North American Standard for Cold-Formed Steel Framing – Lateral Design." Washington, DC, USA.
- American Iron and Steel Institute (AISI) (2012). "AISI S100-12, North American Specification for the Design of Cold-Formed Steel Structural Members." Washington, DC, USA.
- American Iron and Steel Institute (AISI) (2016). "AISI S100-16, North American Specification for the Design of Cold-Formed Steel Structural Members." Washington, DC, USA.
- American Iron and Steel Institute (AISI) (2015). "AISI S400-15, North American specification for seismic design of cold-formed steel structural systems." Washington, DC, USA.
- American Institute of Steel Construction (AISC) (2010). "AISC 341-10, Seismic provisions for structural steel buildings", Chicago, IL, USA.
- American National Standards Institute(ANSI)/American Institute of Steel Construction(AISC) (2010). "ANSI/AISC 360-10, Specification for Structural Steel Buildings." Chicago, IL, USA.
- Ziemian, R. D. (Ed.). (2010). "Guide to stability design criteria for metal structures." *John Wiley & Sons*.
- Branston, A., Chen, Y. C. , Boudreault, F. A. , and Rogers, C. A. (2006). "Testing of light-gauge steel-frame—Wood structural panel shear walls." *Can. J. Civ. Eng.*, 33(5), 561–572.
- Al-Kharat, M., and Rogers, C. A. (2007). "Inelastic performance of cold-formed steel strap braced walls." *J. Constr. Steel Res.*, 63(4), 460–474.
- Ong-Tone, C. (2009). "Tests and Evaluation of Cold-Formed Steel Frame/Steel Sheathed Shear Walls." Project Report, Dept. of Civil Engineering and Applied Mechanics, McGill University, Montreal, QC, Canada.

- Rogers, C.A., Balh, N., Ong-Tone, C., Shamim, I., DaBreo, J. (2011). "Development of Seismic Design Provisions for Steel Sheathed Shear Walls." ASCE/SEI Structures Congress, Las Vegas, USA, 676-687.
- Balh, N. (2010). "Development of Seismic Design Provisions for Steel Sheathed Shear Walls." M.Eng. thesis, Department of Civil Engineering and Applied Mechanics, McGill University, Montreal, QC, Canada.
- Balh, N., DaBreo, J., Ong-Tone, C., El-Saloussy, K., Yu, C., and Rogers, C. A. (2014). "Design of steel sheathed cold-formed steel framed shear walls." *Thin-Walled Struct.*, 75, 76–86.
- DaBreo, J. (2012). "Impact of Gravity Loads on the Lateral Performance of Cold-Formed Steel Frame / Steel Sheathed Shear Walls." M.Eng. thesis, Department of Civil Engineering and Applied Mechanics, McGill University, Montreal, QC, Canada.
- Shamim, I. (2013) "Seismic design of lateral force resisting cold-formed steel framed (CFS) structures." PhD thesis, Department of Civil Engineering and Applied Mechanics, McGill University, Montreal.
- Shamim, I., & Rogers, C. A. (2013) "Steel sheathed/CFS framed shear walls under dynamic loading: numerical modelling and calibration." *Thin-Walled Structures*, 71, 57-71.
- Yu, C., Vora, H., Dainard, T., Tucker, J., Veetvkuri, P. (2007). "Steel Sheet Sheathing Options for Cold-Formed Steel Framed Shear Wall Assemblies Providing Shear Resistance." Report No. UNT-G76234, American Iron and Steel Institute, Department of Engineering Technology, University of North Texas, Denton, Texas, USA.
- Yu, C., Yujie Chen, P. (2009). "Steel Sheet Sheathing Options for Cold-Formed Steel Framed Shear Wall Assemblies Providing Shear Resistance - Phase 2." Report No. UNT-G70752, American Iron and Steel Institute, Department of Engineering Technology, University of North Texas, Denton, Texas, USA.
- Rizk, R., Rogers, C.A. (2018) "Higher Strength Cold-formed Steel Framed / Steel Shear Walls For Mid-rise Construction." Project Report, Dept. of Civil Engineering and Applied Mechanics, McGill University, Montreal, QC, Canada.
- Santos, V., Rogers, C.A. (2018) "Higher Capacity Cold-formed Steel Sheathed And Framed Shear Walls For Mid-rise Buildings: Part 1." Project Report, Dept. of Civil Engineering and Applied Mechanics, McGill University, Montreal, QC, Canada.
- Briere, V., Rogers, C.A. (2018) "Higher Capacity Cold-formed Steel Sheathed And Framed Shear Walls For Mid-rise Buildings: Part 2." Project Report, Dept. of Civil Engineering and Applied Mechanics, McGill University, Montreal, QC, Canada.
- Blais C. (2006) "Testing and Analysis of Light Gauge Steel Frame/9mm OSB Wood Panel Shear Walls" Master's Thesis, Department of Civil Engineering and Applied Mechanics, McGill University, Montreal.
- Leng, J., Peterman, K. D., Bian, G., Buonopane, S. G., & Schafer, B. W. (2017) "Modeling seismic response of a full-scale cold-formed steel-framed building." *Engineering Structures*, 153, 146-165.
- Kechidi, S., & Bourahla, N. (2016) "Deteriorating hysteresis model for cold-formed steel shear wall panel based on its physical and mechanical characteristics." *Thin-Walled Structures*, 98, 421-430.
- Yu, C., Yu, G., & Wang, J. (2015) "Optimization of Cold-Formed Steel Framed Shear Wall Sheathed with Corrugated Steel Sheets: Experiments and Dynamic Analysis." *In Structures Congress 2015* (pp. 1008-1020).
- Comeau, G. (2008) "Inelastic performance of welded CFS strap braced walls." thesis, Department of Civil Engineering and Applied Mechanics, McGill University, Montreal, QC, Canada.
- Hung Huy Ngo. (2014) "Numerical and experimental studies of wood sheathed cold-formed shear walls." M.Eng. thesis, John Hopkins University, Baltimore, United States.
- Zeynalian, M., & Ronagh, H. R. (2012) "A numerical study on seismic performance of strap-braced cold-formed steel shear walls." *Thin-walled structures*, 60, 229-238.
- Zeynalian, M. (2015) "Numerical Study on Seismic Performance of Cold Formed Steel Sheathed Shear Walls." *Advances in Structural Engineering*, 18(11), 1819-1829.
- Buonopane, S. G., Bian, G., Tun, T. H., & Schafer, B. W. (2015) "Computationally efficient fastener-based models of cold-formed steel shear walls with wood sheathing." *Journal of Constructional Steel Research*, 110, 137-148.
- Bian, G., Padilla-Llano, D. A., Leng, J., Buonopane, S. G., Moen, C. D., & Schafer, B. W. (2015) "OpenSees modeling of cold-formed steel framed wall system." *Proceedings of 8th International Conference on Behavior of Steel Structures in Seismic Areas*.
- Tao, F., Cole, R., & Moen, C. D. (2016) "Monotonic and cyclic backbone response of single shear sheathing-to-cold-formed steel screw-fastened connections." Project Report, Department of Civil and Environmental Engineering, Virginia Polytechnic Institute and State University, Blacksburg, VA, USA.
- Mojtabaei, S. M., Kabir, M. Z., Hajirasouliha, I., & Kargar, M. (2018) "Analytical and experimental study on the seismic performance of cold-formed steel frames." *Journal of Constructional Steel Research*, 143, 18-31.